

## NO<sub>x</sub> Control Using Variable Exhaust Valve Timing and Duration

2010-01-1204

Published  
04/12/2010

Ali Mohammad Pourkhesalian, Amir Hossein Shamekhi and Farhad Salimi  
K.N.Toosi Univ. of Technology

Copyright © 2010 SAE International

### ABSTRACT

As it is well known one of the most harmful emissions in SI engines is NO<sub>x</sub> and there are several ways to minimize NO<sub>x</sub> emission. Internal exhaust gas recirculation (IGR) is an effective way to control and minimize NO<sub>x</sub> concentration in exhaust gas. In this paper, a method for minimizing NO<sub>x</sub> emission by use of IGR and variable valve timing (VVT) is introduced. In this method, formation of NO<sub>x</sub> is controlled by mass fraction of residual gas (RG) and mass fraction of RG is controlled by variable timing of exhaust valves opening and closing so not only the timing of exhaust valves changes but also the lift profile of exhaust valves is variable. In this paper, first a thermodynamic model of a SI engine was developed and validated by experimental data. The model was a reliable tool for predicting engine performance and emission characteristics. The effect of variable exhaust valve timing on RG mass fraction, NO<sub>x</sub> formation and brake specific fuel consumption was investigated. Then a multi-objective genetic algorithm (NSGA II) was applied to find the optimum timing and lift duration of exhaust valve.

### INTRODUCTION

A variable valve timing (VVT) mechanism is used to optimize performance and emission of internal combustion engines (ICEs). It can be used for both intake and exhaust valves to control the gas flow into or out of the cylinder. Also, VVT can be used to maximize volumetric efficiency at high speeds or it can be used to control residual gas mass fraction to diminish formation of NO<sub>x</sub> and reduce brake specific fuel consumption. Variable exhaust valve timing could make the exhaust process faster and easier to increase power and torque or it can hinder exhaust process in order to reduce emissions. Despite the fact that variable valve lift mechanism is not currently widely used in vehicular applications, using this mechanism will be definitely

inevitable in the future by use of hydraulic and solenoid valves. Much research has been performed around VVT mechanisms.

Taylor examined the effect of exhaust and intake valve timings on performance characteristics of ICE [1]. Asmus investigated the effect of opening and closure points of both intake and exhaust valves on engine performance [2]. Haugen et.al designed and practiced a VVT system on intake valve. After experimental works they declared that the designed system could increase power and decrease engine fuel consumption [3]. Lancefield et.al in their paper explained using VVT mechanism could decrease fuel consumption and emission in low speeds and increase power and torque in high speeds [4]. Hanato et.al developed a new multi-mode VVT mechanism that performed in three different cases: 1. Deactivate both intake and exhaust valves when low power and speed is needed. 2. Moderate lifts and short durations in low speeds 3. High lifts and long durations in high speeds. Hanato concluded with that VVT mechanism a reduction in fuel consumption of 16% during the Japanese test driving cycle and a power increase by 20% [5]. Leone practiced different valve timing strategies to reduce NO<sub>x</sub> and fuel consumption [6]. Kohany and Sher developed and validated a two-zone model. They used the 2nd law of thermodynamics to optimize valve timing for maximizing engine power and torque [7]. Moro et.al introduced a possible strategy to realize an original engine load control by means of both intake and exhaust VVT [8]. Bozza et.al developed a one-dimensional model and validated it with experimental results. Bozza then, investigated the effect of both intake and exhaust valve timings on performance and emission characteristics of a SI engine but he did not apply any optimization [9]. Golcu et.al used neural networks for the estimation of performance and fuel consumption of a SI engine using different initial valve timings and engine speeds [10]. Alkidas reviewed recent advancements made in gasoline engines for reduction of fuel

consumption and emissions, and the technologies associated with these advancements. Alkidas remarked that flexible valve actuation was a key technology for decreasing fuel consumption and emission of ICEs [11]. Atashkari et.al used artificial neural network and evolutionary algorithms to achieve optimum intake valve timing [12]. Salimi et.al examined the effect of spark advance, air/fuel ratio and valve timing on performance and emissions of a hydrogen fueled engine [13].

In this paper, a thermodynamically quasi-dimensional two-zone model is developed in Matlab and then it is validated by experimental results. The model is capable of estimating engine performance and emissions characteristics with various valve timings and engine speeds. Data achieved from simulations is used to train an artificial neural network and then a multi-objective genetic algorithm method is used to find optimal exhaust valve timings at different engine speeds.

## MODELING

The engine model is a quasi-dimensional two-zone model which solves the basic differential equations for the intake, compression, power and exhaust strokes. In this model, the combustion chamber is divided into two zones by flame front. First zone contains unburned mixture and the second one contains burned mixture. Thermal NOx formation also takes place in burned zone, which is described by the extended Zeldovich mechanism [14]. The flame front is assumed to travel by a speed called turbulent flame speed which is a function of laminar flame speed. The engine model uses Woschni correlation [15] to estimate engine heat transfer. It is assumed that the flame travels in a sphere like shape. The engine model also includes a friction model to predict brake mean effective pressure [16]. The composition of the reaction products is calculated from the chemical equilibrium at a given pressure and temperature of the 12 species N<sub>2</sub>, NO, N, CO<sub>2</sub>, CO, OH, H, O<sub>2</sub>, O, H<sub>2</sub>O, H<sub>2</sub>, Ar. Finally, using Newton - Raphson method, the molar fraction of each species and total mole fraction was calculated [17].

## MODEL FORMULATION

The basic equation for the engine model that is derived from 1st law of thermodynamics is:

$$dE = -\delta Q - \delta W + \sum_i h_i dm_i \quad (1)$$

Where,  $E$  is the internal energy of the cylinder gas mixture,  $Q$  is the heat exchange of the cylinder contents with the cylinder walls where,  $W$  is the work,  $h_i$  is the specific enthalpy of gas which enters or leaves the cylinder, and  $dm_i$

is the mass flow into (+) or out of (-) the cylinder.  $\delta W$  can be expressed as  $P.dv$ , where,  $P$  is the pressure and  $V$  is the cylinder volume [14].

### Intake and Exhaust Processes

The mass flow rate through a valve is usually described by the equation for compressible flow through a flow restriction. This equation is derived from a one-dimensional isentropic flow analysis, and real gas flow effects are included by means of an experimentally determined discharge coefficient,  $C_D$ . The air flow rate is related to the upstream stagnation pressure  $P_o$  and stagnation temperature  $T_o$ , static pressure just downstream of the flow restriction (assumed equal to the pressure at the restriction,  $P_T$ ), and a reference area  $A_R$  characteristic of the valve design [14]:

$$\dot{m} = \begin{cases} \frac{C_D A_R P_o}{(RT_o)^{\frac{1}{2}}} \left(\frac{P_T}{P_o}\right)^{\frac{1}{\gamma}} \left\{ \frac{2\gamma}{\gamma-1} \left[ 1 - \left(\frac{P_T}{P_o}\right)^{\frac{\gamma-1}{\gamma}} \right] \right\}^{\frac{1}{2}} & \text{if } \frac{P_T}{P_o} > \left[ \frac{2}{\gamma+1} \right]^{\frac{\gamma}{\gamma-1}} \\ \frac{C_D A_R P_o}{(RT_o)^{\frac{1}{2}}} \gamma^{\frac{1}{2}} \left(\frac{2}{\gamma+1}\right)^{\frac{\gamma+1}{2(\gamma-1)}} & \text{if } \frac{P_T}{P_o} \leq \left[ \frac{2}{\gamma+1} \right]^{\frac{\gamma}{\gamma-1}} \end{cases} \quad (2)$$

For flow into the cylinder through an intake valve,  $P_o$  is the intake system pressure and  $P_T$  is the cylinder pressure. For flow out of the cylinder through an exhaust valve,  $P_o$  is the cylinder pressure and  $P_T$  is the exhaust system pressure. Several different reference areas can be used. In this paper, the so-called valve curtain area was used as reference area:

$$A_R = \pi D_v L_v \quad (3)$$

Also lift profile is obtained using Ashhab et.al formulation [18].

### Compression and Expansion Strokes

During combustion and expansion equation (1) can be simplified to:

$$\frac{dT}{d\theta} = \frac{1}{mc_v} \left[ -\frac{dQ}{d\theta} - P \frac{dV}{d\theta} + \frac{dm_i}{d\theta} RT \right] \quad (4)$$

Where,  $R$  is the mixture gas constant,  $\theta$  is the crank angle  
 $\frac{dm_l}{d\theta}$   
 and  $\frac{dm_l}{d\theta}$  is the cylinder mass leakage due to blowby. By  
 neglecting the change in gas constant during expansion the  
 rate of pressure change can be calculated from the ideal gas  
 state equation [14,16]:

$$\frac{dP}{d\theta} = \frac{1}{V} \left[ \frac{dm_l}{d\theta} RT + mR \frac{dT}{d\theta} - P \frac{dV}{d\theta} \right] \quad (5)$$

### Combustion Stroke

Using conservation of mass and energy and the ideal gas  
 equation the rate of change of cylinder pressure, unburned  
 and burned gas temperature  $T_u$  and  $T_b$  are:

$$\begin{aligned} \frac{dP}{d\theta} = & \left( \frac{c_{v,u}}{c_{p,u}} - \frac{c_{v,b}}{R_b} \frac{R_u}{c_{p,u}} V_u + \frac{c_{v,b}}{R_b} V \right)^{-1} - \dots \\ & - \left( 1 + \frac{c_{v,b}}{R_b} \right) P \frac{dV}{d\theta} - c_{p,b} T_b \frac{dm_{l,b}}{d\theta} - \frac{R_u}{R_b} c_{p,b} T_u \frac{dm_{l,u}}{d\theta} - \dots \\ & - \left[ (e_b - e_u) - c_{v,b} \left( T_b - \frac{R_u}{R_b} T_u \right) \right] \frac{dm_b}{d\theta} + \left( \frac{c_{v,u}}{c_{p,u}} - \frac{c_{v,b}}{R_b} \frac{R_u}{c_{p,u}} \right) \frac{dQ_u}{d\theta} - \frac{dQ}{d\theta} \end{aligned} \quad (6)$$

Where, subscripts  $u$  and  $b$  denote unburned and burned  
 properties respectively and subscript  $l$ , denotes leakage (due  
 to blowby). Also,  $c_v$  and  $c_p$  are the specific heats at constant  
 volume and pressure respectively,  $i$  is the specific energy  
 $\frac{dm_b}{d\theta}$   
 and  $\frac{dm_b}{d\theta}$  is the mass burning rate, which is derived from a  
 turbulent flame speed model [19].

$$\frac{dT_u}{d\theta} = \frac{1}{m_u c_{p,u}} \left( V_u \frac{dP}{d\theta} - \frac{dQ_u}{d\theta} \right) \quad (7)$$

$$\frac{dT_b}{d\theta} = \frac{P}{m_b R_b} \left[ \frac{dV}{d\theta} - \left( \frac{V_b}{m_b} - \frac{V_u}{m_u} \right) \frac{dm_b}{d\theta} + \frac{V_b}{m_b} \frac{dm_{l,b}}{d\theta} + \frac{V_u}{m_u} \frac{dm_{l,u}}{d\theta} + \left( \frac{V}{P} - \frac{R_u V_u}{c_{p,u} P} \right) \frac{dP}{d\theta} + \frac{R_u}{c_{p,u} P} \frac{dQ_u}{d\theta} \right] \quad (8)$$

Also, the mass burning rate is assumed that:

$$\frac{dm_b}{d\theta} = \rho_u A_f u_t \quad (9)$$

Where;  $\rho$  is density,  $A_f$  is the flame front area and  $u_t$  is the  
 turbulent flame speed.

### Laminar Flame Speed of Gasoline

The burning velocity gasoline can be calculated from  
 Metghalchi and Keck formulation [14]. Their correlation is  
 defined as following.

$$u_l = u_{l,0} \left( \frac{T_u}{T_0} \right)^\alpha \left( \frac{P}{P_0} \right)^\beta (1 - 2.06x_b^{0.77}) \quad (10)$$

Where;  $T_0 = 298 \text{ K}$  and  $P_0 = 1(\text{atm})$  are the reference  
 temperature and pressure, and  $u_{l,0}$ ,  $\alpha$  and  $\beta$  are functions  
 of equivalence ratio for a given fuel, and  $x_b$  is unburned gas  
 diluent fraction. These constants can be represented as  
 follows:

$$\alpha = 2.18 - 0.8(\phi - 1) \quad (11)$$

$$\beta = -0.16 + 0.22(\phi - 1) \quad (12)$$

$$u_{l,0} = B_m + B_\phi (\phi - \phi_m)^2 \quad (13)$$

For gasoline  $\phi_m$ ,  $B_m$  and  $B_\phi$  are 1.21, 0.305 ( $m/s$ ) and  
 $-0.549$  ( $m/s$ ), respectively.

### Turbulent Flame Speed

Various methods for describing and calculating the turbulent  
 flame speed have been developed. In this paper ‘‘Damkohler  
 and derivatives’’ method is used [20, 21]. According to this  
 model turbulent flame speed is calculated as follows:

$$u_t = u' + u_l \quad (14)$$

Where:

$$u' = u'_{TDC} \left( 1 - 0.5 \frac{\theta - 360}{45} \right) \quad (15)$$

$$u'_{TDC} = 0.75 \bar{U}_p \quad (16)$$

$\theta$  is the crank angle (360 at TDC of compression).

## MODEL VALIDATION

In order to validate the developed model, some experiments had been already conducted [22, 23]. The tested engine was Mazda 2000bi. Engine specifications are listed in [table 1](#). The gasoline properties used for experiments are listed in [table 2](#).

**Table 1. Engine specifications**

Engine type	Four stroke, Spark ignition, naturally aspirated, without EGR
Number of cylinders	Four in line
Bore (mm)	86
Stroke (mm)	86
Connecting rod length (mm)	153
Compression ratio	8.6
Maximum power	70 (kw) @ 5000 (rpm)
Maximum torque	151 (N.m) @ 2500 (rpm)
Valve per cylinder	3
Intake valve opening (IVO)	10 BTDC
Intake valve closing	49 ABDC
Maximum intake valve lift (mm)	5.6
Exhaust valve opening	55 BBDC
Exhaust valve closing	12 ATDC
Maximum exhaust valve lift (mm)	5.6

**Table 2. Gasoline properties**

Formula	$C_{7.56}H_{15.5}$
Molecular Weight	106.22
Density ( $kg/m^3$ )	750
Heat of vaporization @298K ( $kJ/kg$ )	305
Lower Heating Value ( $MJ/kg$ )	44.0
Stoichiometric Air/Fuel Ratio	14.6
Research Octane Number	95.8

In [Fig. 1](#), predicted in-cylinder pressure is compared to experimental data. As it can be seen simulated and experimental data match quite well. All the tests and simulations are performed at full-load, wide open throttle (WOT). Spark timings that are used in model has been selected according to their calibrated values saved in electronic control unit (ECU).

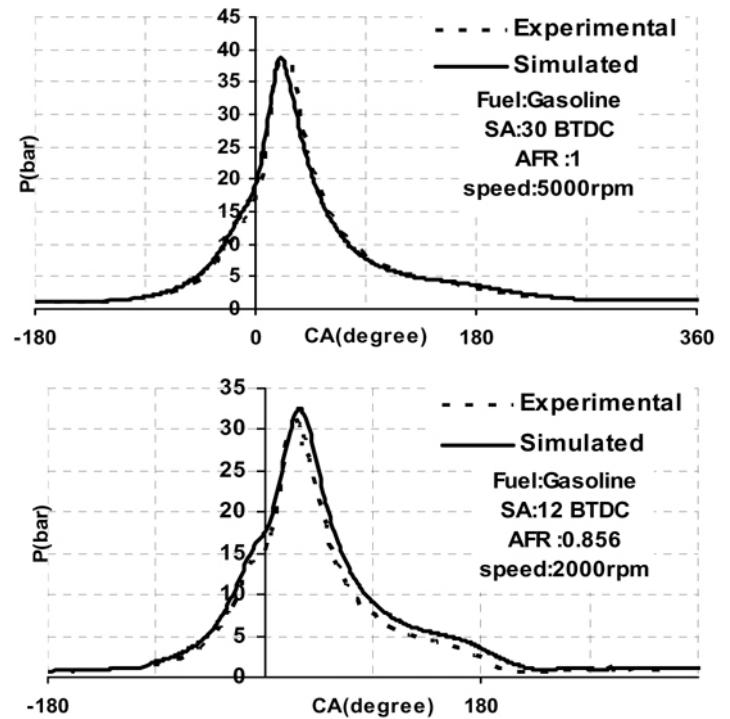


**Fig.1. Comparison between simulated and experimental data.**

In [Fig. 2](#) and [Fig. 3](#) volumetric efficiency, brake specific NO<sub>x</sub> (bsNO<sub>x</sub>) and brake mean effective pressure (BMEP) that are calculated with the model are compared to experimental data. In [Fig.2](#) around the engine speed of 4500 volumetric efficiency reaches its maximum and then decreases because of high pressure loss and choking in high engine speeds. In [Fig. 2](#) and [Fig. 3](#) there are some differences between experimental and simulated data due to simplifications and unmodeled dynamics.

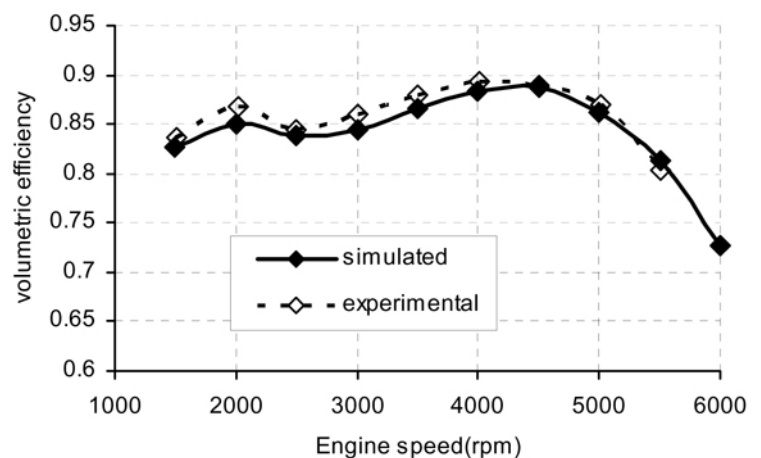


**Fig. 2. volumetric efficiency comparison**

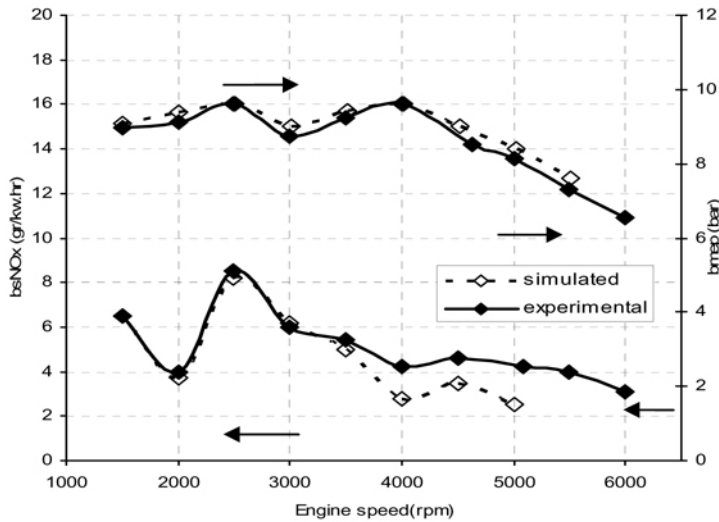


**Fig. 3. bsNOx and bmep comparison**

In Figs. 4 and 5 effect of variation of EVC on mass fraction of residual gases, brake power and NOx concentration are illustrated. EVO is set to 55 bBDC, engine speed is 3000 (rpm), Spark advance is 22 bTDC and equivalence ratio is 1.16. RG mass fraction at EVC=320 stands at approximately 0.11. It must be mentioned when EVC occurs early; exhaust gases do not have enough time to leave the cylinder. As EVC happens later with respect to CA, mass fraction of RG decreases because there is sufficient time for burned gases to leave the cylinder. If EVC happens even later, overlap time of intake and exhaust valves increases and it will cause a steady increment in RG mass fraction.

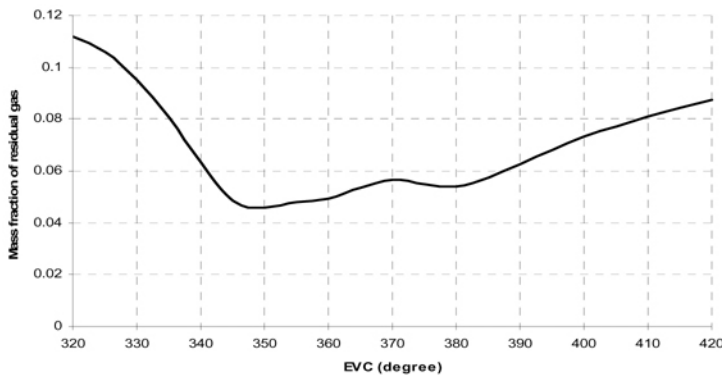


**Fig. 4. Effect of EVC variations on RG mass fraction**

Mass fraction of residual gas influences volumetric efficiency, concentration of in-cylinder mixture and specific heat of in-cylinder mixture. As RG mass fraction increases, volumetric efficiency and concentration of in-cylinder charge decreases and specific heat of in-cylinder charge increases. So an increment in RG mass fraction will result in lowering brake power and NOx formation. In Fig. 5 it is shown that

when RG mass fraction is high, power and NOx concentration are low and vice versa.

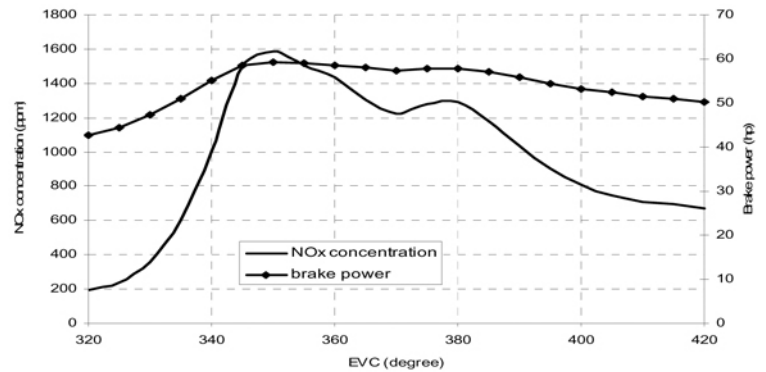


**Fig. 5. Effect of EVC variations on NOx concentration and brake power**

## NEURAL NETWORK

After validating the developed model, it ran with several different exhaust valve timings in a wide range of engine speeds. The exhaust valve opening (EVO) varies in the range of 100 to 200 degree of crank angle (CA) and the exhaust valve closure (EVC) varies from 320 to 420 degree of CA. Due to the engine model runs slow, the optimization algorithm calculation is enormous and ease of applying optimization methods on neural networks, an artificial neural network (ANN) is developed using simulated data.

The neural network used in this paper is feed forward. A back propagation method is used to train the network and the neuron activation function is hyperbolic tangent. Network error is calculated by mean square error method. Many different ANN with various numbers of hidden layers and nodes was checked in order to find an efficient neural network. ANN used in this research has one input layer with two nodes, two hidden layers each with forty nodes and one output layer with 3 nodes. Input variables are EVO and EVC timings and output variables are torque, NOx concentration and brake specific fuel consumption (BSFC). A schematic of the network is shown in Fig. 6.

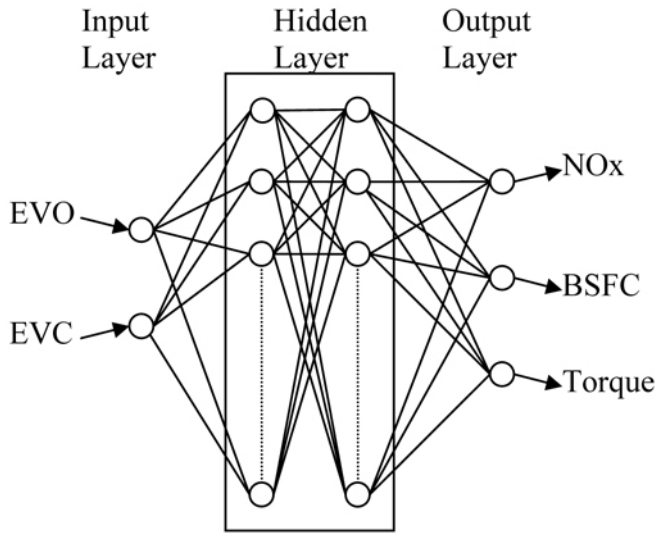


Fig. 6. Schematic of neural network

Eight separate networks are developed in engine speeds of 1500, 2000, 2500, 3000, 3500, 4000, 4500 and 5000 (rpm). For each engine speed 11025 samples are used for developing the network. 75% of samples are used to train the network and the rest of the samples are stored for testing the ANN. In Fig. 7, the simulated data and data achieved from neural network are compared at 3000 (rpm). It can be seen that the neural network results and simulation code results are have good correlation.

<figure 7 here>

## OPTIMIZATION

Optimization in mathematics is defined as maximizing and minimizing of functions. Generally a multi-objective optimization problem (MOP) is defined as to find the vector  $\bar{X}$  to optimize the function  $F(\bar{X})$  which is subjected to  $m$  inequality and  $P$  equality constrains:

$$\bar{X} = [x_1, x_2, x_3, \dots, x_n]^T$$

$$F(\bar{X}) = [f_1(\bar{X}), f_2(\bar{X}), f_3(\bar{X}), \dots, f_k(\bar{X})]^T$$

$$g_i(\bar{X}) \leq 0, \quad i = 1, 2, 3, \dots, m$$

$$h_j(\bar{X}) = 0, \quad j = 1, 2, 3, \dots, p$$

Various optimization methods are introduced by scientists. In this paper, a Pareto based, multi-objective genetic algorithm method is used to find the optimal set of decision vectors. The Pareto approach can be explained with following definitions:

Pareto dominance: vector  $\bar{U} = [u_1, u_2, u_3, \dots, u_k]$  dominant to vector  $\bar{V} = [v_1, v_2, v_3, \dots, v_k]$  (denoted  $\bar{U} < \bar{V}$ ) if and only if there is at least one  $u_j$  that is smaller than  $v_j$  while the remaining  $u$ 's are either smaller or equal to corresponding  $v$ 's.

Pareto optimality: A point  $X^*$  is said to be a Pareto optimal if and only if  $F(\bar{X}^*) < F(\bar{X})$

Parto set: For a given multi-objective optimization problems (MOP), a Pareto set  $P$  is a set in the decision variable space consisting of all the Pareto optimal vectors.

Pareto front: For a given MOP, the Pareto front is a set of vectors of objective functions that are obtained using the vectors of decision variables in the Pareto set  $P$  [24, 25, 26, 27 and 28].

In this paper NSGA-II method is used to find Pareto optimal set and Pareto front. Genetic algorithms have been widely used for multi-objective optimization because of their natural properties suited for these types of problems. This is mostly because of their parallel or population based search approach. Another advantage of evolutionary algorithms is that they calculate real amount of function instead of function derivatives and gradients. Therefore, genetic algorithms provide a simple pervasive search and most of the difficulties and deficiencies within the classical methods in solving multi-objective optimization problems are removed. For example, there is no need for several runs to find the Pareto front or quantification of the importance of each objective using numerical weights. The Pareto based approach of NSGA-II [28, 29] has been used recently in a wide area of engineering MOPs because of its simple yet efficient non-dominance ranking procedure in yielding different level of Pareto frontiers.

After applying NSGA II, Pareto front was found at different engine speed. Decision variables are opening and closing points of exhaust valve and objective functions are NOx concentration, brake torque and brake specific fuel consumption. Fig. 8, illustrates Pareto fronts for 3000 (rpm) engine speed. In table 3, the Pareto front points for 3000 (rpm) engine speed are listed.

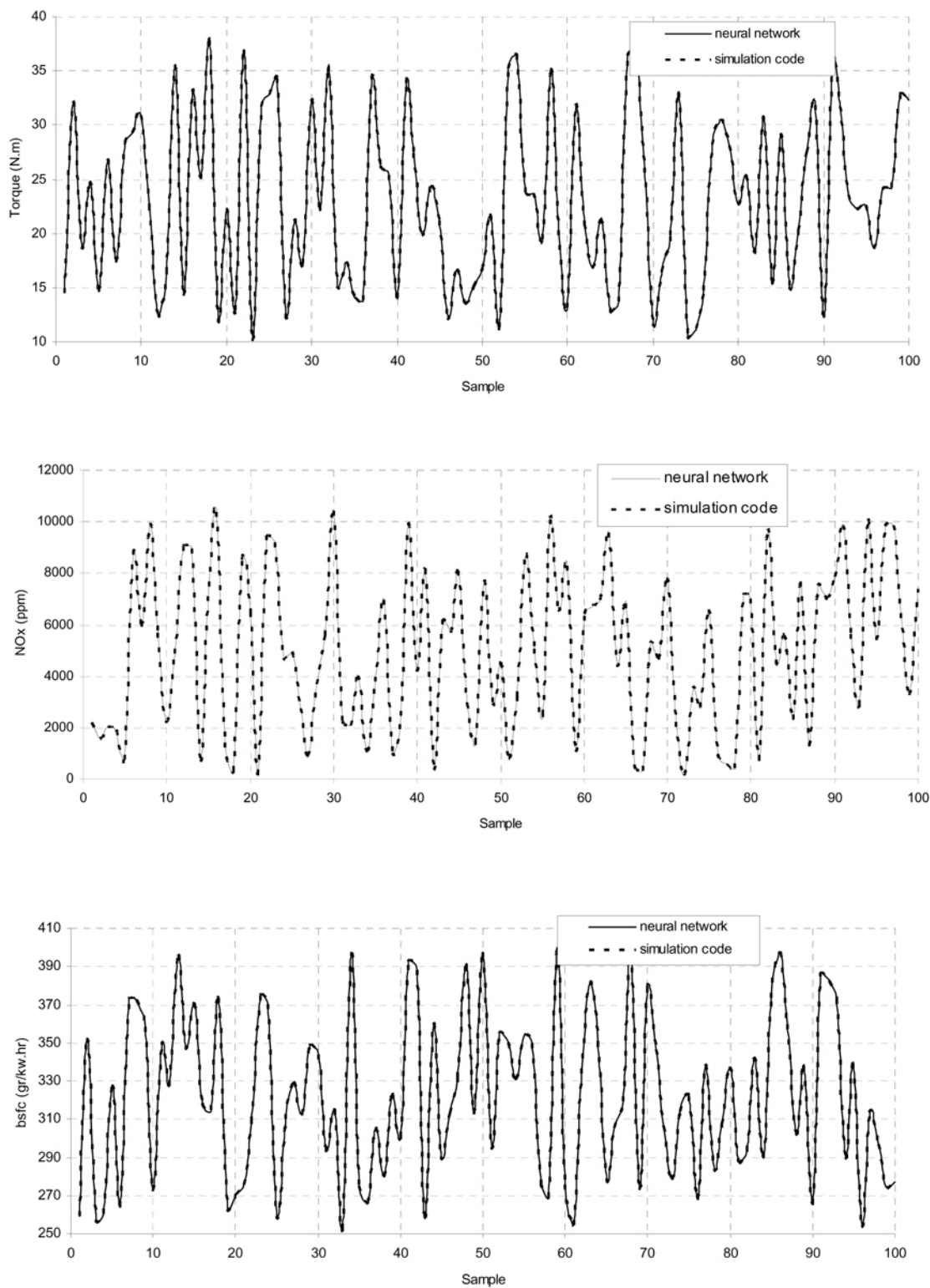


**Fig.7. Comparison between neural network and computer code results**

**Table 3. optimal exhaust valve timings for 3000 (rpm) engine speed at WOT**

Duration (deg)	EVO (deg)	EVC (deg)	Torque (N.m)	NOx (ppm)	BSFC (gr/kw-hr)
208	152	360	147.1	1931	324
198	150	348	135.1	1049	331
203	137	340	127.3	738	337
213	134	347	139.8	1426	327
208	133	341	129.8	884	335
199	151	350	137.5	1192	329
197	133	330	111.4	303	357
206	151	357	146.6	1875	324
185	160	345	127.5	677	338
190	164	354	138	1231	330
180	154	334	118.1	391	348
212	135	347	139.4	1391	327
189	131	320	102.8	195	374
201	136	337	121.3	523	344
200	168	368	147.8	2182	326

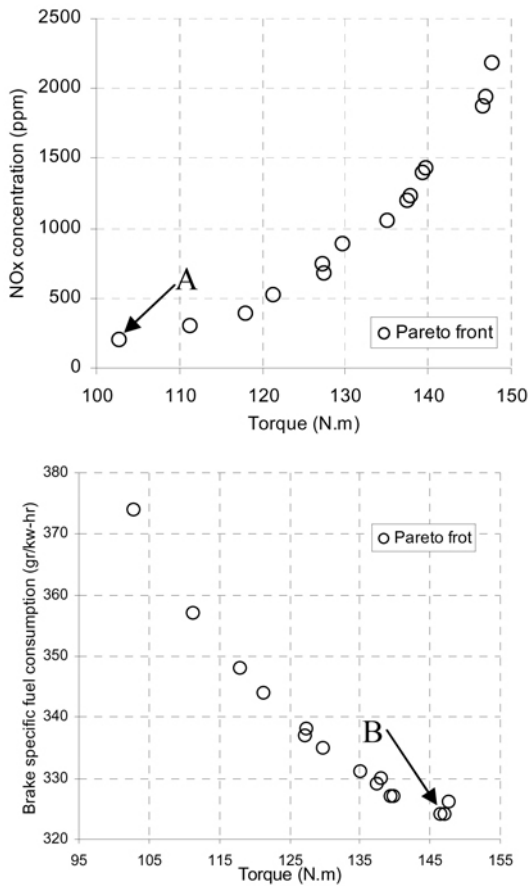


**Fig. 8. Pareto fronts for 3000 (rpm)**

emission” design “point A” could be selected and in a “low fuel consumption” design, “point B” is meritorious.

## DESIGN

In this section two sets of exhaust valve timings are proposed that can adjust engine performance in two different situations. As mentioned, all the tests and simulations are performed at full-load, wide open throttle. The conventional engine did not have external EGR mechanism

### Low Emission

In table 4, the exhaust valve timings which minimize NOx emission can be seen. In Fig. 9, comparison between conventional engine and EVVT engine is shown. Engine with EVVT experienced averagely 71% decrement in NOx emission in exhaust gas. It must be mentioned that the “conventional” curve is obtained using experimental data and the “EVVT” curve is achieved from simulation.

<table 4 here>

<table 3 here>

It must be mentioned that every point on a Pareto front, has equal value. They are all optimal points. No point is better than the others. But in a specific design, the designer can select the proper point. For example in Fig. 8, in a “low



**Table 4. Exhaust valve timings for low emission design at WOT**

Speed (rpm)	Duration (deg)	EVO (deg)	EVC (deg)	Torque (N.m)	NOx (ppm)	BSFC (gr/kw-hr)
1500	209	186	395	103.9	895	335
2000	180	147	327	104.2	233	358
2500	168	161	329	119.6	569	325
3000	189	131	320	102.8	195	374
3500	175	157	332	104.6	177	376
4000	194	138	332	105	77	458
4500	194	148	342	112.2	218	435
5000	294	114	408	112	78	477

**Table 5. Exhaust valve timings for low brake specific fuel consumption design at WOT**

Speed (rpm)	Duration (deg)	EVO (deg)	EVC (deg)	Torque (N.m)	NOx (ppm)	BSFC (gr/kw-hr)
1500	221	146	367	142.6	2078	320
2000	239	146	385	144.1	1156	320
2500	223	149	372	151.2	2383	303
3000	208	152	360	147.1	1931	324
3500	236	138	374	148.2	1063	342
4000	267	118	385	141.4	897	395
4500	214	153	367	141.1	1319	390
5000	235	138	373	144	636	422

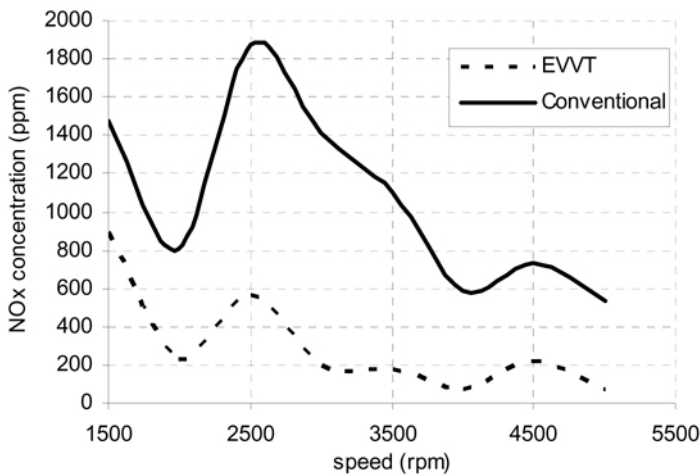


**Fig. 9. Effect of EVVT mechanism on NOx concentration**

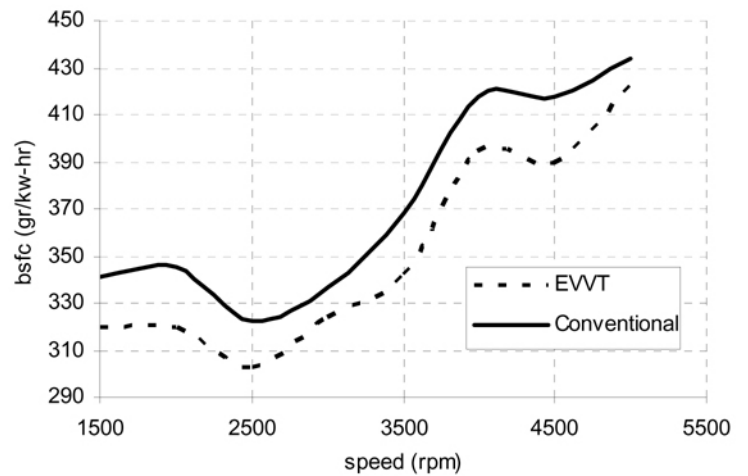


**Fig. 10. Effect of EVVT mechanism on Brake specific fuel consumption**

### Low Brake Specific Fuel Consumption

Using exhaust valve timings proposed in [table 5](#) causes an average reduction in brake specific fuel consumption by 6%.

<[table 5](#) here>

As noted, the “conventional” curve is experimental results and the “EVVT” curve is achieved from simulation.

## CONCLUSION

In this paper, performance and emission characteristics of a SI engine are optimized using variable exhaust valve timing and lift mechanism.

First, a thermodynamically, quasi-dimensional, open-cycle model of an SI engine is developed. Then the developed simulation model is validated by experimental data. Next, an artificial neural network is developed based on simulation results. Then, the neural network performance is checked by test data.

The effect of variable valve timings and lift on RG mass fraction is discussed. Moreover, the influence of RG mass fraction on NOx concentration and brake power is explained.

A multi-objective genetic algorithm method (NSGA II) is used to find the Pareto optimal frontiers in different engine speeds. Design variables are opening and closing timings of exhaust valve and objective functions are NOx concentrations, brake specific fuel consumption and torque.

Using (NSGA II) the Pareto frontiers are found for different engine speeds. After finding Pareto fronts, optimal exhaust valve timings are proposed for two different engine working cases:

1. Low brake specific fuel consumption, at which the target of optimization is to minimize the brake specific fuel consumption
2. Low NOx emission which the target is to diminish the NOx concentration in exhaust gas.

It is concluded, using EVVT would result in a decrease in NOx emission and brake specific fuel consumption. The average reduction of NOx concentration and brake specific fuel consumption are 71 and 6%, respectively.

## REFERENCES

1. Taylor, C. F., *The Internal Combustion Engine in Theory and Practice*, Vol. 1, Chpt 6, M.I.T. Press, Cambridge, MA, 1960.
2. Asmus, T. W., *Effect of Valve Events on Engine Operation*, in *Fuel Economy in Road Vehicles Powered by Spark Ignition Engines*, Hilliard J.C. and Springer G.S, Eds., Plenum Press, New York, NY, 1984.
3. Haugen, D. J., Blackshear, P. L., Piphoo, M. J., Esler, W., "Modifications of a Quad 4 Engine to Permit Late Intake Valve Closure," SAE Technical Paper [921663](#), 1992.
4. Lancefield, T. M., Gayler, R. J., Chattopadhyay, A., "The Practical Application and Effects of a Variable Event Valve Timing System," SAE Technical Paper [930825](#), 1993.
5. Hatano, K., Iida, K., Higashi, H., Murata, S., "Development of a New Multi-mode Variable Valve Timing Engine," SAE Technical Paper [930878](#), 1993.
6. Leone, T. G., Christenson, E. J., Stein, R. A., "Comparison of Variable Camshaft Timing Strategies at Part Load," SAE Technical Paper [960584](#), 1996.
7. Kohany, T. and Sher, E., "Using the 2nd Law of Thermodynamics to Optimize Variable Valve Timing for Maximizing Torque in a Throttled SI Engine," SAE Technical Paper [1999-01-0328](#), 1999.
8. Moro, D., Ponti, F. and Serra, G., "Thermodynamic Analysis of Variable Valve Timing Influence on SI Engine Efficiency," SAE Technical Paper [2001-01-0667](#), 2001.
9. Bozza, F., Gimelli, A., Senatore, A. and Caraceni, A., "A Theoretical Comparison of Various VVA Systems for Performance and Emission Improvements of SI Engines," SAE Technical Paper [2001-01-0670](#), 2001.
10. Mustafa Golcu, Yakup Sekmen, Sahir Erduranli Perihan Salman M., Artificial neural-network based modeling of variable valve-timing in a spark-ignition engine, *Applied Energy*, Vol. 81, 187-219, 2005.
11. Alkidas, Alex. C., *Combustion Advancements in Gasoline Engines*, Energy Conversion and Management, Vol. 48, 2751-2761, 2007.
12. Atashkari K., Nariman-Zadeh N., Golcu M., Khalkhali A., Jamali A., Modeling and multi-objective optimization of a variable valve-timing spark-ignition engine using polynomial neural networks and evolutionary algorithms, *Energy Conversion and Management* Vol. 48, 1029-1041, 2007.
13. Farhad Salimi, Shamekhi Amir H., Pourkhesalian Ali M., Role of mixture richness, spark advance and valve timing in hydrogen-fuelled engine performance and emission, *International Journal of Hydrogen Energy*, Vol. 34, 3922-3929, 2009.
14. Heywood J.B., *Internal Combustion Engine Fundamentals*, McGraw-Hill, 1988.
15. Woschni, G., "A Universally Applicable Equation for the Instantaneous Heat Transfer Coefficient in the Internal Combustion Engine," SAE Technical Paper [670931](#), 1967.
16. Ferguson Colin R. and Kirkpatrick Allan T., *Internal Combustion Engines: Applied Thermoscience*. 2nd Ed, John Wiley & Sons Inc, 2001.
17. Shamekhi A.H., *Simulation and Fuzzy Spark Advance Control in SI engines by Ion Current Sensing*, PhD Thesis, Department of Mechanical Engineering, K. N. Toosi University of Technology, September, 2004.
18. Ashhab, M.S., Stefanopoulou, A.G., Cook, J.A., and Levin, M. Control-Oriented Model for Camless Intake Process-Part 1, *ASME Journal of Dynamic Systems, Measurement, and Control*, Vol 122, 122-130, 2000.
19. Horlock J.H., F.R.S and Winterborn D.E., *The Thermodynamics and Gas Dynamics of Internal Combustion Engines*, Volume II, Clarendon Press, Oxford, 1986.

20. Verhelst S., A study of the combustion in hydrogen-fuelled internal combustion engines, PhD Thesis, Ghent University, Gent, Belgium, 2005.
21. Hall, M. J., Bracco, F. V., "A Study of Velocities and Turbulence Intensities Measured in Firing and Motored Engines," SAE Technical Paper 870453, 1987.
22. Shamekhi A., Khtibzade N., Shamekhi A. H., Performance and emissions characteristics of a bi-fuel SI engine fueled by CNG and gasoline. ASME paper ICES2006-1387, 2006.
23. Pourkhesalian, A. M., Shamekhi, A. H. and Salimi, F., "Performance and Emission Comparison and Investigation of Alternative Fuels in SI Engines," SAE Technical Paper 2009-01-0936, 2009.
24. Coello C.A.C., Lamont G.B. and Van Veldhuizen D.A., Evolutionary Algorithms for Solving Multi-Objective Problems, 2nd Ed, Springer, 2007.
25. Srinivas N, Deb K. Multi-objective optimization using nondominated sorting in genetic algorithms, Evol Comput, Vol. 2, No. 3, 221-248, 1994.
26. Zitzler E., Thiele L., Deb K., Comparison of Multi-objective Evolutionary Algorithms: Empirical Results, Evolutionary Computation, Vol.8, 173-195, 2000.
27. Hiroyasu, T., Miki, M., Kim, M., Watanabe, S., Hiroyasu, H. and Miao, H., "Reduction of Heavy Duty Diesel Engine Emission and Fuel Economy with Multi-Objective Genetic Algorithm and Phenomenological Model," SAE Technical Paper 2004-01-0531, 2004.
28. Deb K, Agrawal S, Pratap A, Meyarivan T. A fast and elitist multi-objective genetic algorithm: NSGA-II, IEEE Trans Evol Comput, Vol. 6, 182-197, 2002.
29. Samadani, E., Shamekhi, Amir H., Behrooz Mohammad H. and Reza Chini, "Pre-Calibration of DI (Direct Injection) Diesel Engine Emissions and Performance Using Neural Network and Multi-Objective Genetic Algorithm", Iranian Journal of Chemistry and Chemical Engineering, IJCCE (Accepted for publication).

<i>atm</i>	Atmosphere
$C_D$	Discharge coefficient
$c_p$	Specifics heat at constant pressure ( $J/kg.K$ )
$c_p$	Specific heat at constant volume ( $J/kg.K$ )
$D_v$	Valve diameter ( $mm$ )
$e$	Specific energy ( $kJ/kg$ )
$E$	Energy ( $J$ )
$h$	Special enthalpy ( $J/kg$ )
$hp$	Horse power ( $hp$ )
$L_v$	Valve lift ( $mm$ )
$m$	Mass ( $kg$ )
$m_l$	Leakage mass (due to blowby) ( $kg/sec$ )
$\dot{m}$	Mass flow rate ( $kg/sec$ )

## DEFINITIONS/ABBREVIATIONS

<b>A/F</b>	Air to Fuel
$A$	Area ( $m^2$ )
$A_R$	Reference area ( $m^2$ )

<b>NO<sub>x</sub></b>	Nitric oxides	$\alpha_T$	Temperature exponent
$P$	Pressure ( $Pa$ )	$\beta_P$	Pressure exponent
$P_0$	Stagnation pressure ( $Pa$ )	$\phi$	Fuel to Air equivalence ratio
<b>Pb</b>	Brake power ( $hp$ )	$\theta$	Crank angle (degree)
$P_T$	Pressure at the restriction ( $Pa$ )	$\gamma$	Specific heat ratio
$Q$	Heat transfer ( $J$ )	$\rho$	Density ( $kg / m^3$ )
$R$	Gas constant ( $kg / kJ.K$ )	<b>Acronyms</b>	
$T$	Temperature ( $K$ )	<b>aBDC</b>	After bottom dead centre
$V$	Volume ( $m^3$ )	<b>AFR</b>	Air/Fuel equivalence ratio
$u$	Burning velocity ( $m / sec$ )	<b>aTDC</b>	After top dead centre
$u'$	Root mean square turbulent velocity ( $m / sec$ )	<b>BDC</b>	Bottom dead centre
$\bar{U}_p$	Mean piston speed ( $m / sec$ )	<b>bmep</b>	Brake mean effective pressure
$W$	Work transfer ( $J$ )	<b>bsfc</b>	Brake specific fuel consumption
		<b>bsNO<sub>x</sub></b>	Brake specific NO <sub>x</sub>
		<b>bTDC</b>	Before top dead centre

<b>CA</b>	Crank angle	<b>SIM</b>	Simulated
<b>ECU</b>	Electronic control unit	<b>TDC</b>	Top Dead Centre
<b>EGR</b>	Exhaust gas recirculation	<b>VVT</b>	Variable valve timing
<b>EVC</b>	Exhaust valve closing	<b>WOT</b>	Wide open throttle
<b>EVO</b>	Exhaust valve opening	<b>Subscripts</b>	
<b>EXP</b>	Experimental	<b>0</b>	Reference condition
<b>GA</b>	Genetic algorithm	<b><i>b</i></b>	Burned
<b>ICE</b>	Internal combustion engine	<b><i>f</i></b>	Flame
<b>IGR</b>	Internal exhaust gas recirculation	<b><i>l</i></b>	Laminar
<b>IVO</b>	Intake valve opening	<b><i>t</i></b>	Turbulent
<b>MOP</b>	Multi-objective optimization problem	<b><i>u</i></b>	Unburned
<b>PPM</b>	Particles per million		
<b>RON</b>	Research octane number		
<b>RPM</b>	Revolution per minute		
<b>SA</b>	Spark advance		
<b>SI</b>	Spark Ignition		

---

The Engineering Meetings Board has approved this paper for publication. It has successfully completed SAE's peer review process under the supervision of the session organizer. This process requires a minimum of three (3) reviews by industry experts.

All rights reserved. No part of this publication may be reproduced, stored in a retrieval system, or transmitted, in any form or by any means, electronic, mechanical, photocopying, recording, or otherwise, without the prior written permission of SAE.

ISSN 0148-7191

doi:[10.4271/2010-01-1204](https://doi.org/10.4271/2010-01-1204)

Positions and opinions advanced in this paper are those of the author(s) and not necessarily those of SAE. The author is solely responsible for the content of the paper.

**SAE Customer Service:**

Tel: 877-606-7323 (inside USA and Canada)

Tel: 724-776-4970 (outside USA)

Fax: 724-776-0790

Email: [CustomerService@sae.org](mailto:CustomerService@sae.org)

**SAE Web Address:** <http://www.sae.org>

**Printed in USA**